Available online at www.easdprocedia.org
EASD Procedia EURODYN (2020) 1521-1528

EASD Procedia

EURODYN 2020
XI International Conference on Structural Dynamics
M. Papadrakakis, M. Fragiadakis, C. Papadimitriou (eds.)
Athens, Greece, 23–26 November 2020

SUPPRESSION OF VIBRATION TRANSMISSION BETWEEN OSCILLATORS COUPLED WITH AN INERTER-BASED JOINT

Zhuang Dong[1], Jian Yang[1*], Han Meng[2] and Dimitrios Chronopoulos[2]

[1] Department of Mechanical, Materials and Manufacturing Engineering, University of Nottingham Ningbo China, Ningbo 315100, PR China.
Zhuang.Dong@nottingham.edu.cn
Jian.Yang@nottingham.edu.cn

[2] Institute for Aerospace Technology & The Composites Group, University of Nottingham, Nottingham, NG8 1BB, UK.
Han.Meng@nottingham.ac.uk
Dimitrios.Chronopoulos@nottingham.ac.uk

Keywords: Vibration transmission, Inerter, Vibration power flow, Force transmissibility

Abstract. *This paper investigates the dynamic characteristics and vibration transmission behaviour of harmonically forced oscillators coupled via an inerter-based joint. The inerter is a recently proposed passive mechanical element that can be used for vibration suppression purpose. The coupled oscillators represent simplified models for the dominant modes of engineering structures such as beams and plates, while the inerter-based joint serves as the vibration transmission path between the two subsystems. The effects of the inerter on the level of vibration transmission are examined for enhanced design of suppression devices. The steady-state dynamic responses of the oscillators and vibration power flow between them are derived analytically. Vibration transmission between the two subsystems is evaluated by both the force transmissibility and time-averaged vibration power flow transmission. It is shown that the use of the inerter in the joint can reduce force and vibration power flow transmission over a large band of excitation frequencies. It is found that the addition of the inerter can also introduce anti-resonances in the frequency-response curves and in the curves of the force transmissibility, where the vibration transmission can be suppressed at specific excitation frequencies. It is shown that force transmissibility reduces at low frequencies and tends to an asymptotic value as the excitation frequency decreases. These findings provide a better understanding of the effects of inerters in the joint on vibration transmission and benefit future designs of mechanical joints of coupled structures for vibration mitigation purpose.*

ISSN:2311-9020
Peer-review under responsibility of the Organizing Committee of EURODYN 2020.
doi: 10.47964/1120.9123.19386

1 INTRODUCTION

There has been a growing demand for high performance vibration control devices that change the vibration transmission behaviour of dynamical systems to meet specific requirements [1]. Some work considers the use of metamaterials for vibration suppression purpose [2-6]. Recently, a passive mechanical element, the inerter, which can be used to provide inertial coupling such as to modify the dynamic behaviour was proposed [7]. The forces applied to the two terminals of the inerter are proportional to the relative accelerations of the two ends, i.e., $F_b = b(\dot{V}_1 - \dot{V}_2)$, where F_b is the coupling inertial force, b is an intrinsic parameter of the inerter named inertance, $\dot{V}_1$ and $\dot{V}_2$ are the accelerations of the two terminals. Since the introduction of the inerter concept, it has been applied to aircraft landing gear shimmy suppression [8], vehicle suspension systems [9] and building vibration control system [10]. Some studies have also been reported on the performance of inerter-based single degree-of-freedom (DOF) vibration isolators [11], dual-stage isolator [12] and nonlinear inerter-based isolator [13].

In many mechanical systems and engineering structures, subsystems are connected via mechanical or structural joints, the design of which is important to reduce vibration transmission between different parts of the integrated system. For the evaluation of vibration transmission level, the force transmissibility and time-averaged vibration power flow quantities may be used. Vibration power flow analysis (PFA) method is a widely accepted tool to characterize the dynamic behaviour of coupled systems and complex structures [14]. Various PFA approaches have been developed to investigate linear vibration control systems. The power flow characteristics of single-DOF inerter-based isolators [11] and two-DOF inerter-based isolators [12] were also investigated. In recent years, this dynamic analysis approach has been developed to investigate vibration power flow in nonlinear vibration isolation systems [15], in oscillators coupled with a nonlinear interface[16], in coupled nonlinear oscillators [17], nonlinear systems with bilinear stiffness and bilinear damping [18] and in impact oscillator systems [19]. It is accordingly beneficial to examine the effects of inerters from a vibration power flow viewpoint for enhanced designs of inerter-based vibration suppression systems.

This paper investigates the influence of introducing the inerter to a mechanical joint on vibration transmission between coupled oscillators. The steady-state response amplitude, force transmissibility and vibration power flow quantities are obtained. The remaining content of the paper is organized as follows. In Section 2, the coupled oscillator system will be briefly introduced and modelled. Then the force transmissibility of the system will be derived in Section 3. The vibration power flow variables and maximum kinetic energies of the system will be formulated in Section 4. Conclusions are drawn in at the end of the paper.

2 THE COUPLING OSCILLATORS MODEL

In this section, the effects of including an inerter in the joint of coupled oscillators on the dynamics and vibration transmission behaviour are investigated. Figure 1 provides a schematic presentation of the model comprising two subsystems coupled with a mechanical joint characterized by an inerter with inertance b and a spring with stiffness coefficient k_0. Subsystem one is a single-DOF system consisting of a mass m_1 subject to an external harmonic excitation of amplitude f_0 with frequency ω, a viscous damper of damping coefficient c_1, and a linear spring with stiffness coefficient k_1. Subsystem two is another single-DOF system having mass m_2, a viscous damper with damping coefficient c_2, and a linear spring with stiffness coefficient k_2. It is assumed that the masses both move horizontally without frictions and their static equilibrium positions, where $x_1 = x_2 = 0$ and the springs are unstretched, are taking as the reference. The dynamic governing equations of the system could be written as

$$m_1\ddot{x}_1 + c_1\dot{x}_1 + k_1x_1 + f_b + k_0(x_1 - x_2) = f_0e^{\mathrm{i}\omega t}, \tag{1a}$$

$$m_2\ddot{x}_2 + c_2\dot{x}_2 + k_2x_2 - f_b - k_0(x_1 - x_2) = 0, \tag{1b}$$

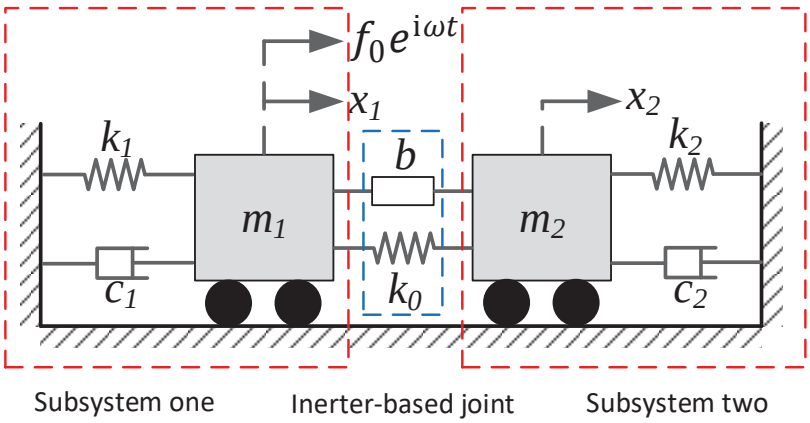

Figure 1: A schematic representation of the coupled oscillator coupled with an inerter-based joint.

where $f_b = b(\ddot{x}_1 - \ddot{x}_2)$, m_i, c_i and k_i $(i = 1, 2)$ are the masses, damping coefficients and spring stiffness coefficients respectively. $x_i, \dot{x}_i$ and $\ddot{x}_i$ $(i = 1, 2)$ represent the displacements, velocities and accelerations respectively. To facilitate later derivations of the response and vibration transmission, the following parameters are introduced

$$\omega_1 = \sqrt{\frac{k_1}{m_1}}, \omega_2 = \sqrt{\frac{k_2}{m_2}}, \mu = \frac{m_2}{m_1}, l_0 = \frac{m_1 g}{k_1}, X_1 = \frac{x_1}{l_0}, X_2 = \frac{x_2}{l_0}, \gamma = \frac{k_2}{k_1}, \delta = \frac{k_0}{k_1},$$

$$\xi_1 = \frac{c_1}{2m_1\omega_1}, \xi_2 = \frac{c_2}{2m_2\omega_2}, \lambda = \frac{b}{m_1}, F_0 = \frac{f_0}{k_1 l_0}, \Omega = \frac{\omega}{\omega_1}, \tau = \omega_1 t,$$

where ω_1 and ω_2 are the undamped natural frequencies of thee subsystems one and two, μ is the mass ratio, l_0 is the characteristic length, X_1 and X_2 are the nondimensional displacements of m_1 and m_2, γ is stiffness ratio of the springs, ξ_1 and ξ_2 are damping ratios, λ is nondimensional inertance ratio, F_0 is nondimensional force amplitude, Ω is the dimensionless excitation frequency and τ is the dimensionless time. Thus, Eq. (1a) and (1b) can be rearranged into the following nondimensional form

$$X_1'' + 2\xi_1 X_1' + X_1 + F_b + \delta(X_1 - X_2) = F_0e^{\mathrm{i}\Omega\tau}, \tag{2a}$$

$$X_2'' + 2\xi_2 X_2' + X_2 - \frac{1}{\gamma}F_b - \frac{\delta}{\gamma}(X_1 - X_2) = 0, \tag{2b}$$

where $F_b = \lambda(X_1'' - X_2'')$. By introducing $X_1 = X_0e^{\mathrm{i}\Omega\tau}, X_2 = Y_0e^{\mathrm{i}\Omega\tau}$, Eq. (2) can be transformed as

$$-\Omega^2 X_0 + 2\xi_1 X_0 \mathrm{i}\Omega + X_0 + \lambda(\Omega^2 Y_0 - \Omega^2 X_0) + \delta(X_0 - Y_0) = F_0, \tag{3a}$$

$$-\Omega^2\gamma Y_0 + 2\xi_2\gamma Y_0 \mathrm{i}\Omega + \gamma Y_0 - \lambda(\Omega^2 Y_0 - \Omega^2 X_0) - \delta(X_0 - Y_0) = 0. \tag{3b}$$

The response amplitudes may be written in the non-dimensional form

$$Y_0 = \frac{\frac{\delta}{\gamma} - \frac{\lambda}{\gamma}\Omega^2}{1 + 2\xi_2 \mathrm{i}\Omega - \Omega^2 - \frac{\lambda}{\gamma}\Omega^2 + \frac{\delta}{\gamma}} X_0, \tag{4a}$$

$$X_0 = \frac{F_0}{1+2\xi_1 \mathrm{i}\Omega-\Omega^2-\frac{1+2\xi_2 \mathrm{i}\Omega-\Omega^2}{1+2\xi_2 \mathrm{i}\Omega-\Omega^2-\frac{\lambda}{\gamma}\Omega^2+\frac{\delta}{\gamma}}(\lambda\Omega^2-\delta)}. \tag{4b}$$

Figure 2 shows the influence of adding the inerter to the mechanical joint on the the response amplitudes of the oscillator masses. Four different values of inertance ratio with $\lambda = 0, 0.5, 1$ and 2 are selected and the corresponding results are shown by solid, dashed, dash-dot and dotted lines. The other parameters are set as $\xi_1 = \xi_2 = 0.02, \gamma = 1, \delta = 1, F_0 = 1$. In the figure, $X = |X_0|$ and $Y = |Y_0|$, denoting the response amplitudes of masses m_1 and m_2, respectively. When the inerter is not included in the joint, two resonant peaks are observed in each curve of X and Y, one of which moves to the lower frequency range with the increase of inertance ratio λ. However, the other peak remains at the same frequency when the inertance ratio λ changes. The anti-peak in Figure 2(a) also moves to low frequency range with the increase of inertance ratio λ. When $\lambda = 1$, two peaks in Figure 2(a) become close with an anti-peak at $\Omega \approx 1$, which indicates the benefit of using inerter for vibration suppression at high frequencies. In Figure 2(b), the addition of inerter introduces an anti-peak in each curve, which can be used to reduce vibration level of mass m_2 at a prescribed excitation frequency.

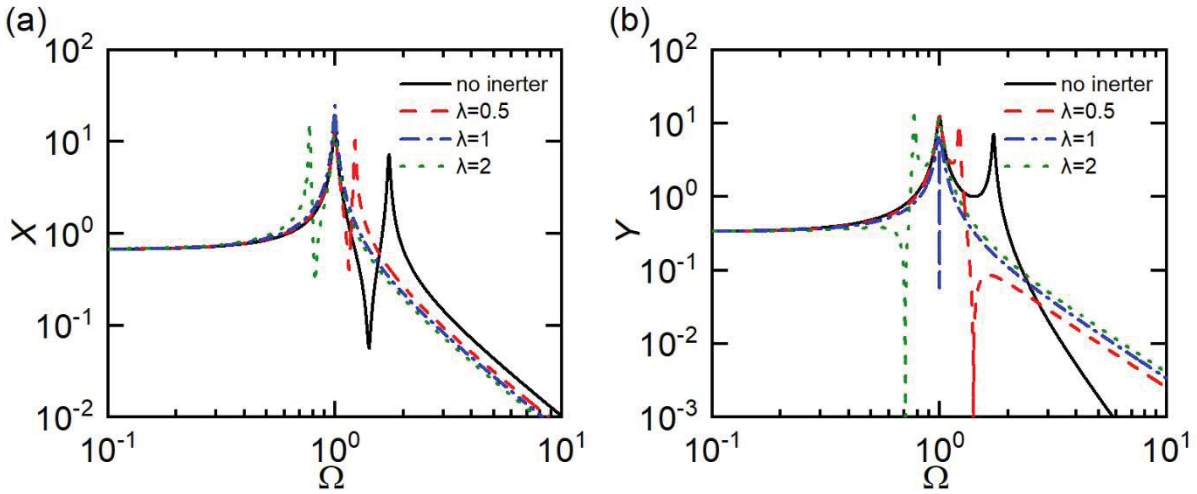

Figure 2: Response amplitude of (a) mass m_1 and (b) mass m_2 ($\xi_1 = \xi_2 = 0.02, \gamma = \delta = F_0 = 1$).

3 FORCE TRANSMISSIBILITY

The force transmissibility has been widely used to evaluate the level of vibration transmission between different subsystems of an integrated structure. It is used here to access the performance of inerter-based mechanical joint in reducing the force transmission. For the current system, the force transmitted to the second mass can be expressed as

$$F_t = F_b + \delta(X_1 - X_2) = \lambda(X_1'' - X_2'') + \delta(X_1 - X_2) = F_{t0}e^{\mathrm{i}\Omega\tau}. \tag{5}$$

As the fore transmissibility is defined as the ratio between the amplitude of the transmitted force and that of the external force, we have

$$TR = \left|\frac{F_{t0}}{F_0}\right| = \left|\frac{\delta-\lambda\Omega^2}{F_0}(X_0 - Y_0)\right|. \tag{6}$$

Figure 3 shows the force transmissibility characteristics of the system with parameters set as $\xi_1 = \xi_2 = 0.02, \gamma = \delta = F_0 = 1$. The figure shows that the use of inerter introduces an anti-peak in each curve, which moves to lower frequency range with the increase of the inertance ratio λ. Figure 3 shows that with the use of inerter in the joint, the force transmissibility TR

remains smaller than 1 in a large range of excitation frequencies. This characteristic can be used to reduce the transmitted force at low excitation frequencies.

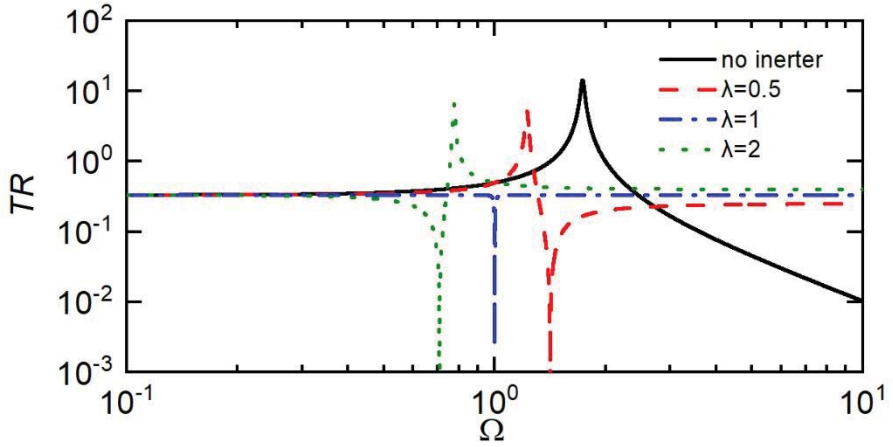

Figure 3: Force transmissibility between oscillators coupled with an inerter-based joint ($\xi_1 = \xi_2 = 0.02, \gamma = \delta = F_0 = 1$).

4 VIBRATION POWER FLOW ANALYSIS

In this section, the vibration transmission behaviour of the inerter-based coupled oscillator system is examined from the perspective of vibration power and energy. The non-dimensional instantaneous input power of the system is the product of the excitation force and the corresponding velocity of the mass

$$P_{in} = F_0 e^{\mathrm{i}\Omega\tau} X_1', \tag{7}$$

where X_1' is the non-dimensional velocity of the mass m_1, which can be expressed as

$$X_1' = \mathrm{i}\Omega X_0 e^{\mathrm{i}\Omega\tau}. \tag{8}$$

Thus, the non-dimensional steady-state time-averaged input power over an excitation cycle is

$$\bar{P}_{in} = \frac{1}{T}\int_{\tau_0}^{\tau_0+T} P_{in}\,\mathrm{d}\tau = \frac{1}{2}\mathrm{Re}\{F_0{}^* X_0 \mathrm{i}\Omega\}, \tag{9}$$

where Re indicates the real part of a complex value and * denotes the complex conjugate. Based on Eq. (4b), the input power for the system can be expressed as

$$\bar{P}_{in} = \frac{1}{2}|F_0^2|\mathrm{Re}\left\{\frac{\mathrm{i}\Omega}{1+2\xi_1\mathrm{i}\Omega-\Omega^2-\frac{1+2\xi_2\mathrm{i}\Omega-\Omega^2}{1+2\xi_2\mathrm{i}\Omega-\Omega^2-\frac{\lambda}{\gamma}\Omega^2+\frac{\delta}{\gamma}}(\lambda\Omega^2-\delta)}\right\}. \tag{10}$$

The corresponding time-averaged transmitted power $\bar{P}_t$ to mass m_2 is

$$\bar{P}_t = \frac{1}{T}\int_{\tau_0}^{\tau_0+T} P_t\,\mathrm{d}\tau = \frac{1}{2}\mathrm{Re}\{F_{t0}{}^* Y_0 \mathrm{i}\Omega\}, \tag{11}$$

The power transmission ratio R_t to mass m_2 may be defined as the ratio between the time-averaged transmitted power $\bar{P}_t$ and the time-averaged input power $\bar{P}_{in}$

$$R_t = \frac{\bar{P}_t}{\bar{P}_{in}}. \tag{12}$$

As the velocity amplitude of mass m_1 in the steady-state motion is $X\Omega$, the non-dimensional maximum kinetic energy of mass m_1 in the steady-state motion is

$$K_{max} = \frac{1}{2}X^2\Omega^2. \tag{13}$$

Based on those formulas, Figure 4 investigates the effects of introducing an inerter-based coupled oscillator on the power flow behaviour. The system parameter values are set as $\xi_1 = \xi_2 = 0.02, \gamma = \delta = F_0 = 1$, the same as those used in Figure 2. Two peaks can be observed in each curve of $\bar{P}_{in}$ and $\bar{P}_t$, Figure 4(a) shows that the use of inerter moves the second peak of $\bar{P}_{in}$ to the low-frequency range with the increase of inertance ratio λ, but corresponding peak value changes little. The first peak frequency and value of $\bar{P}_{in}$ remain almost the same despite of the variations of the inertance ratio λ. The effect of inerter on the time-averaged input power $\bar{P}_{in}$ is relatively small at low and high excitation frequencies. Figure 4(b) shows that the addition of inerter introduces an anti-peak in the curve of time-averaged transmitted power $\bar{P}_t$. The first peak in $\bar{P}_t$ is little affected by the changes of λ. The second peak of $\bar{P}_t$ moves to low frequency range with the increase of inertance ratio λ, but the corresponding peak value remains almost the same. Figure 4(c) plots the variations of the maximum kinetic energy of mass m_1. It shows that for the mechanical joint with inerter, the anti-peak as well as the second peak in the curve without inerter move to the low-frequency range. When $\lambda = 1$, two peaks and one anti-peak merge together as one peak with a higher peak value. This indicates the system in this case is beneficial at high frequencies. The effect of the inerter is little when the frequency is low.

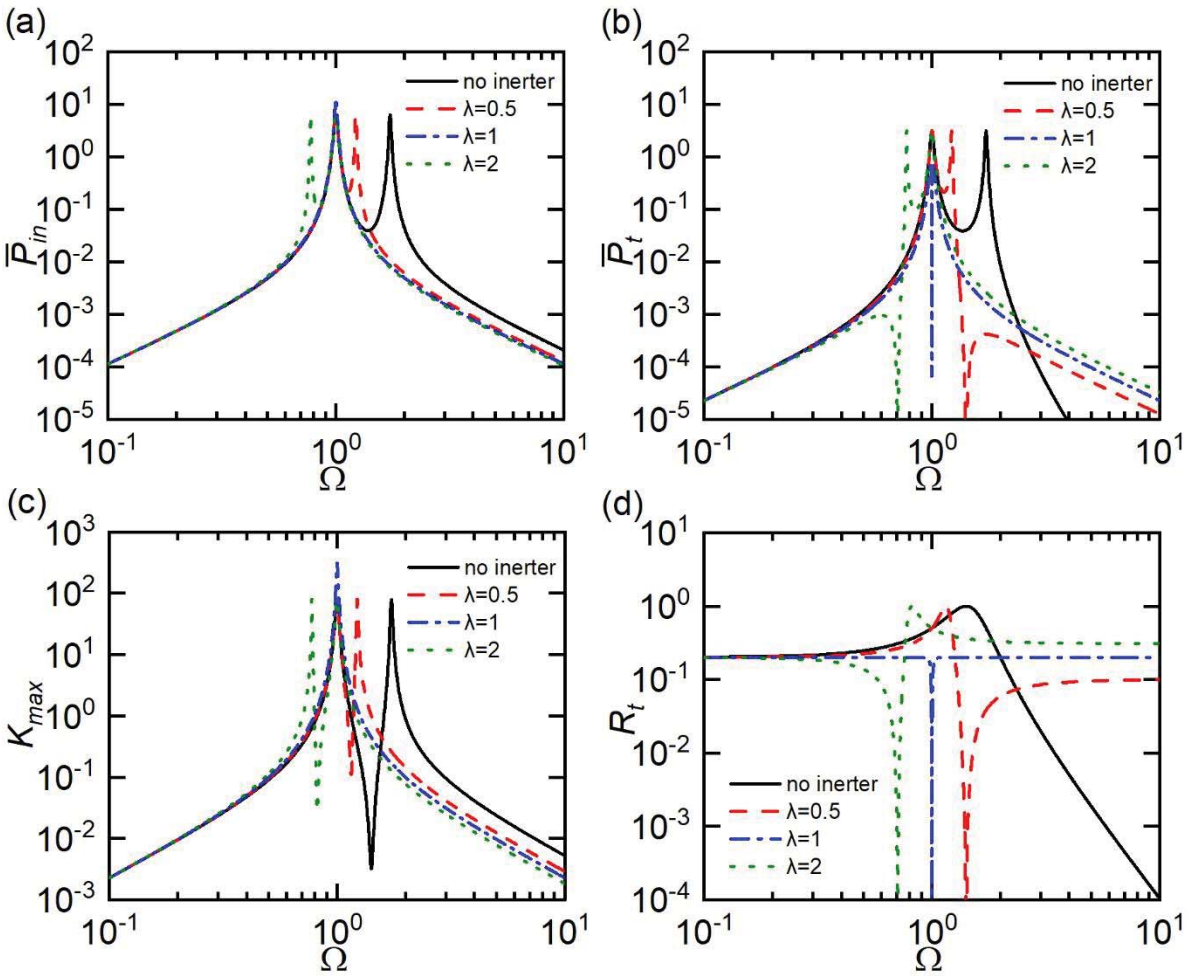

Figure 4: Power flow behaviour of oscillators coupled with an inerter. (a) Time-averaged input power (b) time-averaged transmitted power (c) maximum kinetic energy and (d) power transmission ratio

Figure 4(d) illustrates the influence of inerter in the joint on vibration transmission in terms of the power transmission ratio R_t. An anti-peak is introduced in the curve of R_t, and the peak of the curve moves to the low-frequency range with the increase of inertance ratio λ. When $\lambda = 1$, there is a local minimum point. This characteristic shows the benefits of adding the inerter to the joint at specific excitation frequencies. When Ω is small, the effect of inerter is little, and there is an increase of power transmission ratio R_t with the increase of inertance ratio λ in high frequency range.

5 CONCLUSIONS

The dynamics and performance of an inerter-based mechanical joint between coupled oscillators were investigated in this paper. The force transmissibility and vibration power flow characteristics of the system were examined to evaluate the effects of the inclusion of inerter on the suppression of vibration transmission. It was shown that a larger inertance value leads to a shift of response peaks of the two masses to the low-frequency range. Adding the inerter to the joint results in increases in the force transmission at high excitation frequencies but less time-averaged input power and lower maximum kinetic energy of one of the subsystems. It was found that the inclusion of inerters can provide benefits to vibration mitigation by creating a large frequency band where the force transmissibility and power transmission ratio are relatively low. By properly setting the inertance value, anti-peaks may be created in curves of force transmissibility and power transmission ratio so that their values can be substantially reduced. Based on this property, vibration transmission between the two coupled oscillators can be greatly suppressed at pre-determined excitation frequencies. Asymptotic behaviour of force transmission and power transmission was found when the excitation frequency extends to high frequencies.

ACKNOWLEDGEMENT

This work was supported by National Natural Science Foundation of China (Grant number 51605233) and by Ningbo Science and Technology Bureau under Natural Science Programme (Grant number 2019A610155).

REFERENCES

[1] J. Yang, Y. Xiong and J. Xing (2013). Dynamics and power flow behaviour of a nonlinear vibration isolation system with a negative stiffness mechanism. *Journal of Sound and Vibration*, 332(1), pp.167-183.

[2] H. Meng, D. Chronopoulos, A.T. Fabro, W. Elmadih, I. Maskery, Rainbow metamaterials for broadband multi-frequency vibration attenuation: Numerical analysis and experimental validation, *Journal of Sound and Vibration*, 465, 115005, 2020.

[3] H. Meng, D. Chronopoulos, A.T. Fabro, I. Maskery, Y. Chen, Optimal design of rainbow elastic metamaterials, *International Journal of Mechanical Sciences*, 165, 105185, 2020.

[4] W. Elmadih, D. Chronopoulos, W. Syam, I. Maskery, H. Meng, R. Leach, Three-dimensional resonating metamaterials for low-frequency vibration attenuation, Scien-tific Reports, 9, 1-8, 2019.

[5] O. McGee, H. Jiang, F. Qian, Z. Jia, L. Wang, H. Meng, D. Chronopoulos, Y. Chen, L. Zuo, 3D printed architected hollow sphere foams with low-frequency phononic band gaps, *Additive Manufacturing*, 30, 100842, 2019.

[6] H. Meng, D. Chronopoulos, A.T. Fabro, Numerical simulation data for the dynamic properties of rainbow metamaterials, *Data in brief*, 28, 104772, 2020.

[7] M. Smith (2002). Synthesis of mechanical networks: the inerter. *IEEE Transactions on Automatic Control*, 47(10), pp.1648-1662.

[8] Y. Li, J. Jiang and Neild, S. (2017). Inerter-Based Configurations for Main-Landing-Gear Shimmy Suppression. *Journal of Aircraft*, 54(2), pp.684-693.

[9] J. Jiang, A. Matamoros-Sanchez, R. Goodall and M. Smith (2012). Passive suspensions incorporating inerters for railway vehicles. *Vehicle System Dynamics*, 50(sup1), pp.263-276.

[10] S. Zhang, J. Jiang and S. Neild (2016). Optimal configurations for a linear vibration suppression device in a multi-storey building. *Structural Control and Health Monitoring*, 24(3).

[11] J. Yang, Force transmissibility and vibration power flow behaviour of inerter-based vibration isolators, *Journal of Physics: Conference Series*, 2016, 744(1): 012234.

[12] J. Yang, J. Jiang, X. Zhu and H. Chen (2017). Performance of a dual-stage inerter-based vibration isolator. *Procedia Engineering*, 199, pp.1822-1827.

[13] J. Yang, J. Jiang and S. Neild (2019). Dynamic analysis and performance evaluation of nonlinear inerter-based vibration isolators. *Nonlinear Dynamics*. [online] Available at: https://doi.org/10.1007/s11071-019-05391-x.

[14] H. Goyder and R. White (1980). Vibrational power flow from machines into built-up structures, part III: Power flow through isolation systems. *Journal of Sound and Vibration*, 68(1), pp.97-117

[15] J. Yang, Y. Xiong and J. Xing (2016). Vibration power flow and force transmission behaviour of a nonlinear isolator mounted on a nonlinear base. *International Journal of Mechanical Sciences*, 115-116, pp.238-252.

[16] J. Yang, B. Shi and C. Rudd (2018). On vibration transmission between interactive oscillators with nonlinear coupling interface. *International Journal of Mechanical Sciences*, 137, pp.238-251.

[17] B. Shi and J. Yang (2019). Quantification of vibration force and power flow transmission between coupled nonlinear oscillators. *International Journal of Dynamics and Control*, https://doi.org/10.1007/s40435-019-00560-7.

[18] B. Shi, J. Yang and C. Rudd (2019). On vibration transmission in oscillating systems incorporating bilinear stiffness and damping elements. *International Journal of Mechanical Sciences*, 150, pp.458-470.

[19] W. Dai, J. Yang and B. Shi (2020). Vibration transmission and power flow in impact oscillators with linear and nonlinear constraints. *International Journal of Mechanical Sciences*, 168, p.105234.